Corneal Epithelial Immune Dendritic Cell Alterations in Subtypes of Dry Eye Disease: A Pilot In Vivo Confocal Microscopic Study

Ahmad Kheirkhah,[1] Raheleh Rahimi Darabad,[1] Andrea Cruzat,[1,2] Amir Reza Hajrasouliha,[1] Deborah Witkin,[1] Nadia Wong,[1] Reza Dana,[3] and Pedram Hamrah[1,3,4]

[1]Ocular Surface Imaging Center, Harvard Medical School, Boston, Massachusetts, United States
[2]Department of Ophthalmology, Pontificia Universidad de Chile, Santiago, Chile
[2]Cornea Service, Massachusetts Eye & Ear Infirmary, Department of Ophthalmology, Harvard Medical School, Boston, Massachusetts, United States
[3]Boston Image Reading Center and Cornea Service, New England Eye Center/Tufts Medical Center, Department of Ophthalmology, Tufts University School of Medicine, Boston, Massachusetts, United States

Correspondence: Pedram Hamrah, Boston Image Reading Center and Cornea Service, New England Eye Center/Tufts Medical Center, Department of Ophthalmology, Tufts University School of Medicine, 800 Washington Street, Boston, MA 02111, USA; phamrah@tuftsmedicalcenter.org, p_hamrah@yahoo.com.

Submitted: June 5, 2015
Accepted: September 27, 2015

Citation: Kheirkhah A, Rahimi Darabad R, Cruzat A, et al. Corneal epithelial immune dendritic cell alterations in subtypes of dry eye disease: a pilot in vivo confocal microscopic study. *Invest Ophthalmol Vis Sci*. 2015;56:7179–7185. DOI:10.1167/iovs.15-17433

Purpose. To evaluate density and morphology of corneal epithelial immune dendritic cells (DCs) in different subtypes of dry eye disease (DED) using in vivo confocal microscopy (IVCM).

Methods. This retrospective study included 59 eyes of 37 patients with DED and 40 eyes of 20 age-matched healthy controls. Based on clinical tests, eyes with DED were categorized into two subtypes: aqueous-deficient ($n = 35$) and evaporative ($n = 24$). For all subjects, images of laser scanning in vivo confocal microscopy (IVCM) of the central cornea were analyzed for DC density and DC morphology (DC size, number of dendrites, and DC field). These DC parameters were compared among all dry eye and control groups.

Results. Compared with the controls, patients with DED had significantly higher DC density, larger DC size, higher number of dendrites, and larger DC field (all $P < 0.001$). Comparison between aqueous-deficient and evaporative subtypes demonstrated that DC density was significantly higher in aqueous-deficient subtype (189.8 ± 36.9 vs. 58.9 ± 9.4 cells/mm^2, $P = 0.001$). However, there were no significant differences in morphologic parameters between DED subtypes. When aqueous-deficient DED with underlying systemic immune disease (Sjögren's syndrome and graft versus host disease) were compared with nonimmune conditions, the immunologic subgroup showed significantly higher DC density, DC size, and number of dendrites (all $P < 0.05$).

Conclusions. Corneal IVCM demonstrated differential changes in DC density and morphologic DC parameters between subtypes of DED. These changes, which reflect the degree of immune activation and inflammation in DED, can be used for clinical practice and endpoints in clinical trials.

Keywords: dry eye disease, in vivo confocal microscopy, inflammation, dendritic cells

Dry eye disease (DED) is one of the most commonly encountered ophthalmic disorders. It is a multifactorial disease of the ocular surface and tear film, characterized by symptoms of eye irritation, tear instability, and vision impairment.[1] In addition to evaluating symptoms, a variety of clinical tests are currently being used to diagnose DED, including the Schirmer's wetting test, tear break-up time (TBUT), tear osmolarity, and vital dye staining of the ocular surface by fluorescein, Rose Bengal and Lissamine Green. However, complex clinical features of the disease make the diagnosis a challenge in many cases.[2,3] Therefore, there remains a significant need for objective tests, which can be used to accurately diagnose DED and/or monitor therapeutic response in DED and its underlying changes.

Recent studies have shown that the immune changes play an important role in the pathogenesis of DED.[4] One of the major players in immune system is antigen-presenting cells (APCs), which induce T-cell activation, resulting in inflammatory cascade in DED.[5–7] Although in the ocular surface a variety of cells such as monocytes and macrophages may act as APCs, corneal dendritic cells (DCs) have been demonstrated to be crucial for the DED pathogenesis.[4,8–10] Therefore, evaluation of these cells in patients with DED may provide a better insight to the underlying changes of the clinical manifestations.

To evaluate changes in DCs in patients with DED, corneal in vivo confocal microscopy (IVCM) has lately been used. In vivo confocal microscopy is a noninvasive imaging modality that enables studying the cornea at a cellular level.[11–14] With IVCM, all cellular structures, including epithelial DCs in the cornea, can be clearly visualized, and have been shown to be consistent with immunohistochemistry findings.[15,16] Using IVCM in patients with DED, recent studies have shown changes in DCs in the corneal subbasal layer.[17–21] However, the extent of DC changes remain unclear in different subtypes of DED.

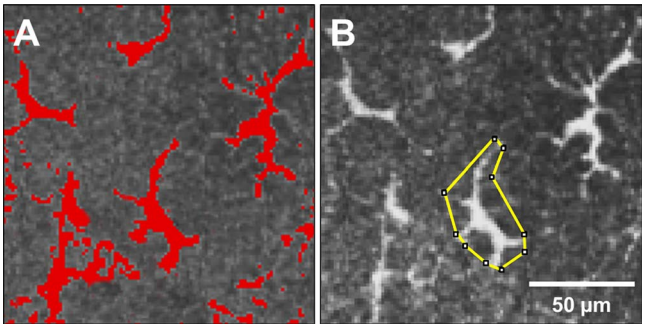

FIGURE 1. Measurement of morphologic parameters of DCs using ImageJ software. The size of DC was measured using the Threshold Function (**A**). The number of dendrites per cell was calculated manually. The DC field was calculated by measuring the area covered by a polygon joining the dendrite tips around each cell (**B**).

Further, while previous studies have revealed changes in DC density, morphologic changes of DC have recently gained attention, as increased size of DCs is a sign of their maturation, activation, MHC-II (HLA-DR) expression, and their antigen presentation capability.[22,23] Thus, recent studies have assessed DC morphology in their evaluation of IVCM changes of the cornea in conditions other than DED.[24–27]

As the level of corneal immune cell activation may vary in different subtypes of DED (aqueous-deficient versus evaporative), we hypothesize that patients with different subtypes of DED will demonstrate differential levels of DC changes not only for DC density, but also for DC morphology.

Materials and Methods

This retrospective, cross-sectional, controlled study included 59 eyes of 37 patients with DED and 40 eyes of 20 age-matched healthy controls. The charts and IVCM images were reviewed for these individuals who had been seen in the Cornea Service of the Massachusetts Eye & Ear Infirmary, Boston, Massachusetts between 2009 and 2012. The protocol of the study was approved by the institutional review board/Ethics Committee, complied with the Health Insurance Portability and Accountability Act (HIPAA) and adhered to the tenets of the Declaration of Helsinki.

All these patients had typical symptoms of DED for a duration of 6 months or more. The patients were categorized to have evaporative DED if they had TBUT less than 10 seconds and Schirmer's test results greater than 5 mm. In the presence of a low Schirmer's test result ($\leq$5 mm) and a low TBUT ($<$10 seconds), the patient was categorized as aqueous-deficient DED. The aqueous-deficient DED group was further stratified into two subgroups, the immunologic subgroup (including cases with Sjögren's syndrome, as defined by American–European consensus group criteria,[28] and graft versus host disease [GVHD]) and the nonimmunologic subgroup. The healthy controls were asymptomatic healthy individuals with a clear healthy cornea without vital staining and normal tear function tests. The exclusion criteria in both groups included active ocular allergy, history of contact lens wear or infectious keratitis in the past 3 months, history of refractive surgery, history of intraocular surgery, or diabetes mellitus.

In Vivo Confocal Microscopy

All patients in both the DED and control groups had undergone imaging with a laser IVCM of the central cornea using Heidelberg Retina Tomograph 3 with the Rostock Cornea Module (Heidelberg Engineering GmbH, Heidelberg, Germany) as previously described.[26] This microscope is equipped with a $\times$63 objective immersion lens with a numerical aperture of 0.9 (Olympus, Tokyo, Japan) and uses a 670-nm red wavelength diode laser source. Each image represents a coronal section of the cornea of 400 $\times$ 400 μm (horizontal $\times$ vertical). Digital images were recorded with the sequence mode at a rate of 3 frames per second, including 100 images per sequence. There was a separation of 1 μm between adjacent images, and a lateral resolution of 1 μm/pixel. A total of six to eight sequence scans of nonoverlapping areas were recorded from the full thickness of the central cornea, with three to four sequence scans focusing on the subbasal layer, resulting in 300 to 400 images of the subbasal layer alone.

Image Analysis

For each eye, three images of epithelial DCs, posterior to the basal epithelial layer and anterior to Bowman's layer, typically at a depth of 50 to 70 μm were chosen for analysis. The criteria to select the images were the best focused, without motion or folds, best contrast, and representing a single layer of the cornea. Dendritic cells were morphologically identified as bright individual dendritiform structures with cell bodies. The following parameters were determined for each image, as elaborated below: DC density, DC size (the area covered by the body of the cell), number of dendrites per DC, and DC field (area bounded within the span of the dendrites).

To evaluate the density and morphologic parameters of DC in IVCM images, ImageJ software (http://imagej.nih.gov/ij/; provided in the public domain by the National Institutes of Health, Bethesda, MD, USA) was used. The density of DC per image was counted using Cell Count tool in the manual mode. All complete DCs present in each image, as well as partial cells on the top and right borders of each frame were counted. The average density of DCs for three images was then calculated. The 10 most representative cells in three images for each eye were then selected for morphologic analysis. The size of DC was measured using the Threshold Function (Fig. 1A). The number of dendrites per cell was calculated manually. The DC field, which is a representative of the cell span and the length of the dendritic processes, was calculated by measuring the area covered by a polygon joining the dendrite tips around each cell (Fig. 1B). Two masked observers (RRD and AC) evaluated all the images and the averaged values were used for the analysis. In case of more than 10% difference between the two observers, a third observer evaluated the images as well and the average of these three values was used for the analysis.

Statistical Analysis

The normal distribution of the data was first confirmed with the Shapiro-Wilk test. Comparison of various clinical and IVCM parameters among different groups were performed using Student's *t*-test and ANOVA with post hoc Bonferroni test. *P* values less than 0.05 were considered as statistically significant. The IVCM data were expressed as mean $\pm$ SEM. The differences found in DC density (the primary endpoint) between the evaporative and aqueous-deficient subtypes were used to calculate the power of the study to detect a statistically significant difference, which was 95%.

Results

This study included 59 eyes of 37 patients with DED (28 females and 9 males) and 40 eyes of 20 heathy controls (14 females and 6 males). The mean age was 58.1 $\pm$ 17.4 years

Investigative Ophthalmology & Visual Science

Table 1. The Clinical Data in Subtypes of DED Compared With the Control Group

	Controls	Evaporative	Aqueous-Deficient	*P* Value
Number of eyes	40	24	35	
Number of patients	20	16	21	
Age, y	57.9 ± 7.6	60.9 ± 15.7	56.9 ± 17.2	0.89
Sex, female/male	14/6	13/3	15/6	0.72

(range, 24–87 years) in the DED group and 57.9 ± 7.6 years (range, 48–74 years) in the control group ($P = 0.93$). The subtypes of DED included, evaporative in 24 eyes, and aqueous-deficient in 35 eyes. The demographic data of these subtypes have been presented in Table 1.

Compared with the control group, the eyes in the DED group had a higher DC density (19.6 ± 2.8 vs. 136.5 ± 23.6 cells/mm^2, respectively, $P < 0.001$, with an average increase of 700%), larger DC size (54.2 ± 1.7 vs. 144.6 ± 14.8 μm^2, respectively, $P < 0.001$, with an average increase of 266%), higher number of dendrites per cell (2.2 ± 0.04 vs. 4.4 ± 0.1, respectively, $P < 0.001$, with an average increase of 200%), and larger DC field (198.0 ± 8.6 vs. 414.7 ± 55.3 μm^2, respectively, $P < 0.001$, with an average increase of 209%; Fig. 2). Table 2 shows the IVCM parameters for DCs in subtypes of DED as compared with the control group. In the aqueous-deficient subtype, DC density and all morphologic parameters (DC size, number of dendrites, and DC field) were significantly higher than the control group (all $P < 0.001$), with average increases of 968%, 284%, 200%, and 224%, respectively. In the evaporative subtype, density of DC as well as DC size and number of dendrites were significantly higher than in the control group ($P < 0.001$, $P = 0.02$, and $P < 0.001$, respectively) with average increases of 300%, 242%, and 191%, respectively. However, the difference in DC field between the evaporative subtype and the control group was not statistically significant ($P = 0.13$), even though there was an average increase of 188%.

Comparison between the aqueous-deficient and evaporative subtypes demonstrated that although DC density was significantly higher in the aqueous-deficient subtype (189.8 ± 36.9 vs. 58.9 ± 9.4 cells/mm^2, $P = 0.001$), there were no significant differences in the morphologic parameters between the two subtypes (Fig. 3).

The aqueous-deficient DED group was further stratified into two subgroups, the immunologic subgroup ($n = 16$) and nonimmunologic subgroup ($n = 19$). The IVCM parameters for DCs for these subgroups have been compared with the evaporative subtype in Table 3. The DC density, DC size, and number of dendrites, but not DC field, were significantly higher in the immunologic subgroup as compared with the nonimmunologic subgroup ($P = 0.004$, $P = 0.04$, $P = 0.04$, $P = 0.15$, respectively; Fig. 4). Further, comparison of these two subgroups with the evaporative subtype showed that although there were no significant differences in any IVCM parameters between the nonimmunologic subgroup and the evaporative subtype, the immunologic subgroup had significantly higher DC density than the evaporative subtype ($P = 0.002$; Fig. 4).

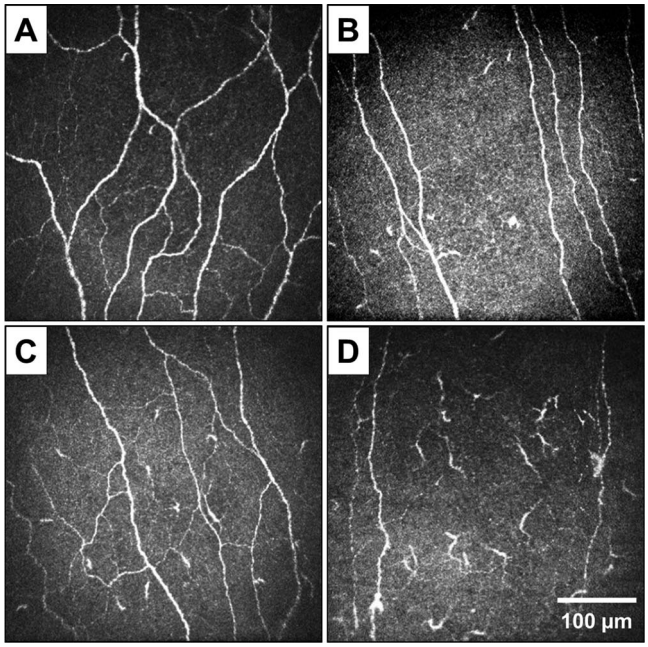

Figure 2. Corneal in vivo confocal microscopy images in normal controls (**A**), evaporative DED (**B**), as well as nonimmunologic (**C**) and immunologic (**D**) subgroups of aqueous-deficient DED demonstrate differential alterations in DC density and morphologic parameters in different subtypes of DED compared with controls.

Discussion

The current study showed that in patients with DED there were significant increases, not only in DC density, but also in all morphologic DC parameters, including cell size, number of dendrites, and cell field. Furthermore, DC density was significantly lower in the evaporative subtype of DED as compared with the aqueous-deficient subtype, suggesting lower degrees of immune activation or inflammation in this subtype of DED. Increased DC activation with higher DC density and larger cells with more dendrites were also noted in cases with underlying systemic autoimmune diseases, such as GVHD and Sjögren's syndrome, as compared with patients with nonimmunologic diseases. These data collectively implicate the utility of IVCM in revealing the underlying immune cell changes in subtypes of DED.[26]

Corneal epithelial immune DCs, including Langerhans cells, are professional antigen-presenting cells, which play a significant role in corneal immune homeostasis. Not only do they have an important role in innate immunity, but they also are major players in the immune surveillance and induction of

Table 2. The In Vivo Confocal Microscopy Parameters for DCs in Subtypes of DED Compared With the Control Group

	Controls, $N = 40$	Evaporative, $N = 24$	Aqueous-Deficient, $N = 35$
DC density, cells/mm^2	19.6 ± 2.8	58.9 ± 9.4*	189.8 ± 36.9*†
DC size, μm^2	54.2 ± 1.7	131.1 ± 29.6*	153.9 ± 14.9*
DC dendrites, number/cell	2.2 ± 0.04	4.2 ± 0.2*	4.4 ± 0.2*
DC field, μm^2	198.0 ± 8.6	372.5 ± 109.5	443.6 ± 56.7*

* $P < 0.05$ compared with the controls.
† $P < 0.05$ compared with the evaporative subtype.

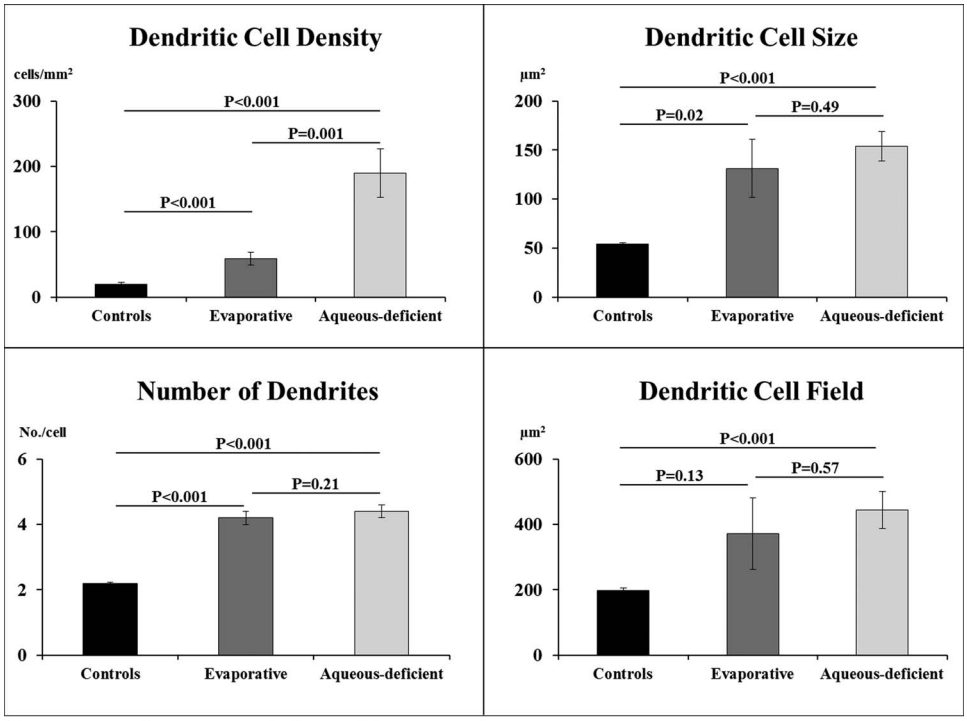

Data are expressed as mean ± standard error of the mean

Figure 3. Dendritic cell density and morphologic parameters in evaporative and aqueous-deficient subtypes of DED as well as the healthy controls. For both the aqueous-deficient and evaporative subtypes, DC density and all morphologic parameters were significantly higher than the control group, except for DC field in the evaporative subtype. Dendritic cell density, but not morphologic parameters, was significantly higher in the aqueous-deficient subtype as compared with the evaporative subtype.

antigen-specific immune reactivity and tolerance.[6,7] Given their established role in immune regulation of the ocular surface,[5–7] there has been a recent interest in evaluation of their alterations in various ocular surface diseases. Recent studies have shown that the DC density significantly increases in various conditions such as DED,[17–21,29] corneal graft rejection,[5,30] contact lens wear,[22,31] and infectious keratitis.[32] In addition to changes in DC density, the morphology of these cells changes upon stimulation, resulting in maturation of these cells with an increase in cell size and formation and lengthening of dendritic processes.[15,16,27,33,34] Evaluation of DC in the clinical setting has recently been facilitated by the fact that they can be easily detected and quantified by laser IVCM,[16,26,35,36] with high interobserver agreement in their quantification ($R = 0.997$; $P < 0.001$).[37]

Using IVCM, although our control group had a DC density within the range reported before, the DED group showed a significantly higher DC density in the central cornea, as has been reported before,[18–21] with an average increase of 700% compared with the age-matched controls. Furthermore, using a detailed morphologic description of DCs, we demonstrated that in DED these immune cells had a larger cell size with increased number and length of dendrites. The average increase in DC size, number of dendrites, and DC field as compared with controls were 266%, 200%, and 209%, respectively. Increased DC size and number of dendrites in DED has also been reported previously using qualitative scales.[18,20,21] However, because DED is a heterogeneous disease with multiple underlying etiologies, we further evaluated the DC changes in subtypes of the disease.

In our study, the evaporative and aqueous-deficient subtypes demonstrated differential degrees of increased DC parameters (Table 2; Fig. 3). Compared with the controls, eyes with both aqueous-deficient and evaporative subtypes had significant increases in DC density and all morphologic parameters, except for DC field in the evaporative group. For the aqueous-deficient and evaporative subtypes, there were mean increases of 968% and 300%, respectively, for DC density, 284% and 242%, for DC size, 200% and 191% for number of dendrites, and 224% and 188% for DC field. Furthermore,

Table 3. The In Vivo Confocal Microscopy DC Parameters in Immunologic (Including GVHD And Sjögren's Syndrome) and Nonimmunologic Subgroups of Aqueous-Deficient DED Compared With the Evaporative DED

	Evaporative, $N = 24$	Aqueous-Deficient Nonimmunologic, $N = 19$	Aqueous-Deficient Immunologic, $N = 16$
DC density, cells/mm²	58.9 ± 9.4	78.6 ± 17.6	239.6 ± 52.9*†
DC size, µm²	131.1 ± 29.6	117.8 ± 17.7	178.9 ± 23.9†
DC dendrites, number/cell	4.2 ± 0.2	4.1 ± 0.2	4.8 ± 0.2
DC field, µm²	372.5 ± 109.6	351.3 ± 81.6	515.7 ± 87.1

* $P < 0.05$ compared to the evaporative subtype.
† $P < 0.05$ compared to the nonimmunologic subgroup of aqueous-deficient subtype.

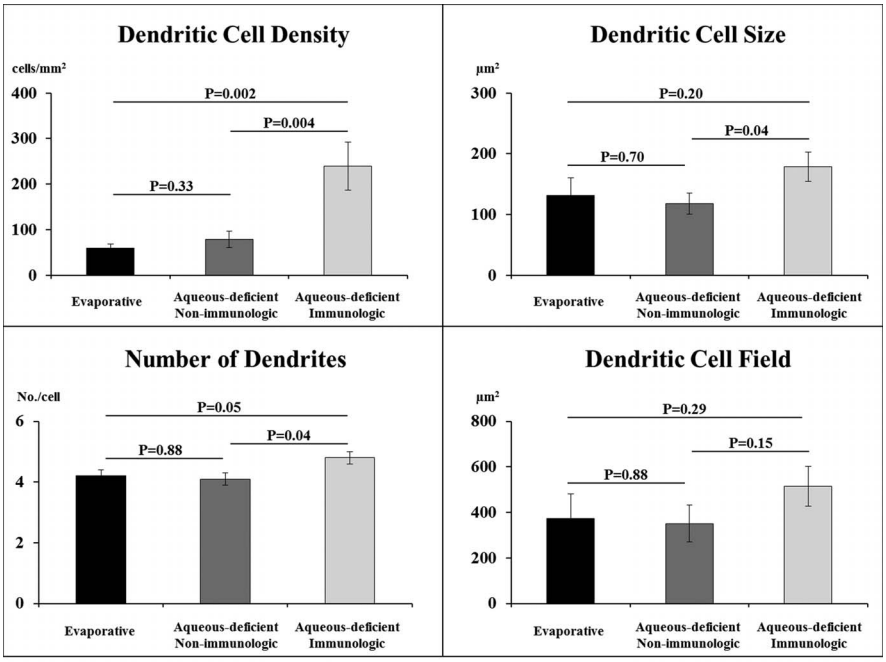

FIGURE 4. Dendritic cell density and morphologic parameters in immunologic and nonimmunologic subgroups of the aqueous-deficient subtype of DED as compared with the evaporative subtype. The DC density, DC size, and number of dendrites, but not DC field, were significantly higher in the immunologic subgroup as compared with the nonimmunologic subgroup. In addition, although there were no significant differences in any IVCM parameters between the nonimmunologic subgroup and the evaporative subtype, the immunologic subgroup had significantly higher DC density and number of dendrites than the evaporative subtype.

comparison of these two subtypes of DED revealed that although DC density and all morphologic parameters were higher in the aqueous-deficient subtype, the difference reached a statistical significance only for the DC density ($P = 0.001$), but not morphologic parameters (Fig. 3). Therefore, although corneal immune changes are seen in both subtypes of DED, the extent of involvement seems to be dependent on the subtype and is more severe in aqueous-deficient eyes. However, because the aqueous-deficient DED itself may be associated with underlying systemic immune diseases, we further investigated the DC alterations in these systemic conditions.

The current study further subdivided eyes with aqueous-deficient DED into two subgroups: with and without underlying systemic immunologic disease such as Sjögren's syndrome and GVHD (Table 3). Interestingly, DC density and morphologic parameters, except for DC field, were significantly higher in eyes with these underlying immunologic conditions (Fig. 4). This is in line with previous data, where increased DC density in eyes with Sjögren's syndrome compared with non-Sjögren's DED has been described.[19] Furthermore, Lin et al.[18] found that although DC density and size increased in the central cornea of DED with and without Sjögren's syndrome, peripheral corneas demonstrated higher DC density and larger DC size only in patients with Sjögren's syndrome. In addition, increased DC density in the cornea and conjunctiva of patients with Sjögren's syndrome compared with non-Sjögren's DED was demonstrated by Wakamatsu and coworkers.[38] Moreover, although changes in corneal DC parameters have not been previously reported in GVHD, an increased DC density has previously been noted in patients with systemic autoimmune diseases such rheumatoid arthritis, ankylosing spondylitis, and Stevens-Johnson syndrome.[20,21,39] Visibility of these immune changes in the cornea may make it possible to assess the activity of immune system and the inflammatory response, and thus help tailor treatment through patient stratification. Interestingly, Villani and colleagues[40] recently showed that in patients who had active rheumatoid arthritis with secondary Sjögren's syndrome, systemic immunosuppression resulted in a significant decrease in corneal DC density, which paralleled the improvement in the ocular symptoms and signs. This further implicates the use of corneal DC parameters to evaluate the efficacy anti-inflammatory therapy for DED in clinical practice and clinical trials. Therefore, this approach may be used as a biomarker in clinical research to evaluate the degree of corneal inflammation in DED and to monitor the therapeutic effect of anti-inflammatory drugs.[41]

Despite demonstrating the utility of DC parameters in subtypes of DED, our current study has several limitations. First of all, although in the Dry Eye Workshop 2007 (DEWS) DED has been divided into aqueous-deficient and evaporative subtypes, the criteria for the distinction between these two have not been clarified by this Workshop.[1] Therefore, since the TBUT was less than 10 seconds in all patients, we have used the Schirmer's test, which is commonly used to measure tear secretion, to categorize the patients into these two subtypes. Our aqueous-deficient subtype in fact had both low Schirmer's test values and low TBUT. Eyes with pure aqueous tear deficiency (normal TBUT) were not included in this study, as this subtype is not commonly encountered. Furthermore, because of the retrospective nature of the study, we could not use any established questionnaire to diagnose the DED; in addition, we did not evaluate the tear film quality in our patients. In addition, we did not investigate the effects of DED severity on the DC density and morphology in different subtypes, as it would require a much larger sample size. Moreover, only the central part of the cornea was evaluated in the current study, and thus the results cannot be extrapolated to the peripheral cornea or the conjunctiva. Previous studies have shown that changes in the central and peripheral cornea in DED may not necessarily parallel each other.[16] Nevertheless, our study

provides, for the first time, a detailed quantitative description of DC morphologic parameters for IVCM images in patients with subtypes of DED, which may aid in the improved assessment of these cells. Thus, the demonstration of differential responses in DC parameters in different subtypes of DED may further elucidate the pathogenesis of this complex disease. While the current study was designed and powered to assess DC density and morphologic features in subtypes of DED, currently a study in a larger cohort of patients with DED is underway to assess the correlation of these DC changes to severity if DED.

In conclusion, there are differential changes in both DC density and morphologic DC parameters between subtypes of DED. These changes, which reflect the degree of immune activation and inflammation in DED, can be detected and quantified objectively by corneal IVCM, allowing its use for clinical practice and clinical trials.

Acknowledgments

Presented in part at the American Academy of Ophthalmology, Chicago, Illinois, United States, October 2011 and the Association for Research and Vision in Ophthalmology, Ft. Lauderdale, Florida, United States, May 2012.

Supported by grants from the National Institutes of Health (Bethesda, MD, USA) K08-EY020575 (PH), New England Corneal Transplant Research Fund (PH; Boston, MA, USA), Falk Medical Research Foundation (PH; Chicago, IL, USA), and Research to Prevent Blindness (PH, RD; New York, NY, USA).

Disclosure: **A. Kheirkhah**, None; **R. Rahimi Darabad**, None; **A. Cruzat**, P; **A.R. Hajrasouliha**, None; **D. Witkin**, None; **N. Wong**, None; **R. Dana**, Allergan (C), P; **P. Hamrah**, Allergan (C), GlaxoSmithKline (C), P

References

1. The definition and classification of dry eye disease: report of the Definition and Classification Subcommittee of the International Dry Eye WorkShop (2007). *Ocul Surf*. 2007;5:75–92.
2. Yokoi N, Komuro A, Maruyama K, Kinoshita S. New instruments for dry eye diagnosis. *Semin Ophthalmol*. 2005; 20:63–70.
3. Bron AJ. Diagnosis of dry eye. *Surv Ophthalmol*. 2001; 45(suppl 2):S221–S226.
4. Stevenson W, Chauhan SK, Dana R. Dry eye disease: an immune-mediated ocular surface disorder. *Arch Ophthalmol*. 2012;130:90–100.
5. Forrester JV, Xu H, Kuffova L, Dick AD, McMenamin PG. Dendritic cell physiology and function in the eye. *Immunol Rev*. 2010;234:282–304.
6. Hamrah P, Dana MR. Corneal antigen-presenting cells. *Chem Immunol Allergy*. 2007;92:58–70.
7. Dana MR. Corneal antigen-presenting cells: diversity, plasticity, and disguise: the Cogan lecture. *Invest Ophthalmol Vis Sci*. 2004;45:722–727.
8. Barabino S, Chen Y, Chauhan S, Dana R. Ocular surface immunity: homeostatic mechanisms and their disruption in dry eye disease. *Prog Retin Eye Res*. 2012;31:271–285.
9. Schaumburg CS, Siemasko KF, De Paiva CS, et al. Ocular surface APCs are necessary for autoreactive T cell-mediated experimental autoimmune lacrimal keratoconjunctivitis. *J Immunol*. 2011;187:3653–3662.
10. Pflugfelder SC, Stern ME. Mucosal environmental sensors in the pathogenesis of dry eye. *Expert Rev Clin Immunol*. 2014; 10:1137–1140.
11. Lemp MA, Dilly PN, Boyde A. Tandem-scanning (confocal) microscopy of the full-thickness cornea. *Cornea*. 1985;4:205–209.
12. Niederer RL, McGhee CN. Clinical in vivo confocal microscopy of the human cornea in health and disease. *Prog Retin Eye Res*. 2010;29:30–58.
13. Erie JC, McLaren JW, Patel SV. Confocal microscopy in ophthalmology. *Am J Ophthalmol*. 2009;148:639–646.
14. Villani E, Baudouin C, Efron N, et al. In vivo confocal microscopy of the ocular surface: from bench to bedside. *Curr Eye Res*. 2014;39:213–231.
15. Knickelbein JE, Buela KA, Hendricks RL. Antigen-presenting cells are stratified within normal human corneas and are rapidly mobilized during ex vivo viral infection. *Invest Ophthalmol Vis Sci*. 2014;55:1118–1123.
16. Mayer WJ, Mackert MJ, Kranebitter N, et al. Distribution of antigen presenting cells in the human cornea: correlation of in vivo confocal microscopy and immunohistochemistry in different pathologic entities. *Curr Eye Res*. 2012;37:1012–1018.
17. Tuisku IS, Konttinen YT, Konttinen LM, Tervo TM. Alterations in corneal sensitivity and nerve morphology in patients with primary Sjögren's syndrome. *Exp Eye Res*. 2008;86:879–885.
18. Lin H, Li W, Dong N, et al. Changes in corneal epithelial layer inflammatory cells in aqueous tear-deficient dry eye. *Invest Ophthalmol Vis Sci*. 2010;51:122–128.
19. Villani E, Magnani F, Viola F, et al. In vivo confocal evaluation of the ocular surface morpho-functional unit in dry eye. *Optom Vis Sci*. 2013;90:576–586.
20. Marsovszky L, Nemeth J, Resch MD, et al. Corneal Langerhans cell and dry eye examinations in ankylosing spondylitis. *Innate Immun*. 2013;20:471–477.
21. Marsovszky L, Resch MD, Nemeth J, et al. In vivo confocal microscopic evaluation of corneal Langerhans cell density, and distribution and evaluation of dry eye in rheumatoid arthritis. *Innate Immun*. 2013;19:348–354.
22. Zhivov A, Stave J, Vollmar B, Guthoff R. In vivo confocal microscopic evaluation of langerhans cell density and distribution in the corneal epithelium of healthy volunteers and contact lens wearers. *Cornea*. 2007;26:47–54.
23. Mastropasqua L, Nubile M, Lanzini M, et al. Epithelial dendritic cell distribution in normal and inflamed human cornea: in vivo confocal microscopy study. *Am J Ophthalmol*. 2006;142:736–744.
24. Eden U, Fagerholm P, Danyali R, Lagali N. Pathologic epithelial and anterior corneal nerve morphology in early-stage congenital aniridic keratopathy. *Ophthalmology*. 2012;119:1803–1810.
25. Fagerholm P, Lagali NS, Ong JA, et al. Stable corneal regeneration four years after implantation of a cell-free recombinant human collagen scaffold. *Biomaterials*. 2014; 35:2420–2427.
26. Cruzat A, Witkin D, Baniasadi N, et al. Inflammation and the nervous system: the connection in the cornea in patients with infectious keratitis. *Invest Obthalmol Vis Sci*. 2011;52:5136–5543.
27. Mayer WJ, Irschick UM, Moser P, et al. Characterization of antigen-presenting cells in fresh and cultured human corneas using novel dendritic cell markers. *Invest Ophthalmol Vis Sci*. 2007;48:4459–4467.
28. Vitali C, Bombardieri S, Jonsson R, et al. Classification criteria for Sjögren's syndrome: a revised version of the European criteria proposed by the American-European Consensus Group. *Ann Rheum Dis*. 2002;61:554–558.
29. Alhatem A, Cavalcanti B, Hamrah P. In vivo confocal microscopy in dry eye disease and related conditions. *Semin Ophthalmol*. 2012;27:138–148.
30. Niederer RL, Sherwin T, McGhee CN. In vivo confocal microscopy of subepithelial infiltrates in human corneal transplant rejection. *Cornea*. 2007;26:501–504.

31. Sindt CW, Grout TK, Critser DB, Kern JR, Meadows DL. Dendritic immune cell densities in the central cornea associated with soft contact lens types and lens care solution types: a pilot study. *Clin Ophthalmol*. 2012;6:511–519.
32. Mocan MC, Irkec M, Mikropoulos DG, Bozkurt B, Orhan M, Konstas AG. In vivo confocal microscopic evaluation of the inflammatory response in non-epithelial herpes simplex keratitis. *Curr Eye Res*. 2012;37:1099–1106.
33. Banchereau J, Steinman RM. Dendritic cells and the control of immunity. *Nature*. 1998;392:245–252.
34. Hamrah P, Huq SO, Liu Y, Zhang Q, Dana MR. Corneal immunity is mediated by heterogeneous population of antigen-presenting cells. *J Leukoc Biol*. 2003;74:172–178.
35. Rosenberg ME, Tervo TM, Muller LJ, Moilanen JA, Vesaluoma MH. In vivo confocal microscopy after herpes keratitis. *Cornea*. 2002;21:265–269.
36. Zhivov A, Stave J, Vollmar B, Guthoff R. In vivo confocal microscopic evaluation of Langerhans cell density and distribution in the normal human corneal epithelium. *Graefes Arch Clin Exp Ophthalmol*. 2005;243:1056–1061.
37. Kheirkhah A, Muller R, Mikolajczak J, et al. Comparison of standard versus wide-field composite images of the corneal subbasal layer by in vivo confocal microscopy. *Invest Ophthalmol Vis Sci*. 2015;56:5801–5807.
38. Wakamatsu TH, Sato EA, Matsumoto Y, et al. Conjunctival in vivo confocal scanning laser microscopy in patients with Sjögren syndrome. *Invest Ophthalmol Vis Sci*. 2010;51:144–150.
39. Vera LS, Gueudry J, Delcampe A, Roujeau JC, Brasseur G, Muraine M. In vivo confocal microscopic evaluation of corneal changes in chronic Stevens-Johnson syndrome and toxic epidermal necrolysis. *Cornea*. 2009;28:401–407.
40. Villani E, Galimberti D, Del Papa N, Nucci P, Ratiglia R. Inflammation in dry eye associated with rheumatoid arthritis: cytokine and in vivo confocal microscopy study. *Innate Immun*. 2013;19:420–427.
41. Villani E, Garoli E, Termine V, Pichi F, Ratiglia R, Nucci P. Corneal confocal microscopy in dry eye treated with corticosteroids. *Optom Vis Sci*. 2015;92:e290–e295.

Investigative Ophthalmology & Visual Science